Journal of Engineering Physics and Thermophysics, Vol. 72, No. 3, 1999

MULTISALT-CARBON CHEMICAL COOLER FOR SPACE APPLICATIONS

L. Vasil'ev, D. Nikanpour,
A. Antukh, K. Snelson,
L. Vasil'ev, Jr., and A. Lebru

UDC 621.577

Introduction. Thermal management systems for future large spacecraft or high-power constellations of small satellites must be able to handle high power densities for final heat ejection into space. Currently, passive radiators or single-phase/two-phase (liquid–vapor) mechanically or capillary pumped systems have been developed as thermal control systems relying on heat by collection through evaporation and heat release by condensation via space radiators.

As an alternative to these thermal control systems, solid sorption thermal machines are currently being considered. These passive thermal machines (coolers, refrigerators, heat pumps, heat transformers) transfer caloric energy from a low-temperature level to a high-temperature level at heat-dissipating stations and radiators for ejection into space.

A good example of application is use for lunar missions where during the day, conventional unshaded space radiators would have to look at either the sun or the hot lunar surface, making heat ejection directly into the environment difficult.

Another example is use for the cooling of electronic components during the lunar or Martian day, when the temperature of the surroundings could be higher than 50 °C or even more. Among solid sorption machines we need to consider liquid/vapor (L/V) equilibrium and solid/gas (S/G) equilibrium [1]. There are three modifications of these systems: the resorption system (2S/G), the internal heat recovery system (1L/V and 2S/G), and the resorption internal heat recovery system (3S/G). Recently a multisalt reactor process was suggested that implements an L/V balance and several S/G equilibria [2].

Following Castaing-Lasvignottes and Neveu [2] for two-salt resorption systems, application of the first and second laws of thermodynamic gives

$$Q^1_{\text{reg}} + Q^1_{\text{abs}} + Q^2_{\text{reg}} + Q^2_{\text{abs}} = 0 ,$$

$$\frac{Q^1_{\text{reg}}}{T^1_{\text{reg}}} + \frac{Q^1_{\text{abs}}}{T^1_{\text{abs}}} + \frac{Q^2_{\text{reg}}}{T^2_{\text{reg}}} + \frac{Q^2_{\text{abs}}}{T^2_{\text{reg}}} + \Delta_i S = 0 . \tag{1}$$

Neglecting internal irreversibilities, for external irreversibilities we have

$$\Delta_i S^{\text{ext}} = \Sigma \left(\int \frac{\delta q_i}{T} - \frac{1}{T_i} \int \delta q_i \right) ;$$

introducing the entropic temperature term as

$$\tilde{T} \equiv \frac{\int \delta q_i}{\int \frac{\delta q_i}{T}}$$

Academic Scientific Complex "A. V. Luikov Institute of Heat and Mass Transfer of the National Academy of Sciences of Belarus," Minsk. Published in Inzhenerno-Fizicheskii Zhurnal, Vol. 72, No. 3, pp. 595-600, May-June, 1999. Original article submitted December 24, 1998.

1062-0125/99/7203-0572$22.00

we obtain the following system:

$$Q^1_{\mathrm{reg}} + Q^1_{\mathrm{abs}} + Q^2_{\mathrm{reg}} + Q^2_{\mathrm{abs}} = 0 ,$$

$$\frac{Q^1_{\mathrm{reg}}}{\tilde{T}^1_{\mathrm{reg}}} + \frac{Q^1_{\mathrm{abs}}}{\tilde{T}^1_{\mathrm{abs}}} + \frac{Q^2_{\mathrm{reg}}}{\tilde{T}^2_{\mathrm{reg}}} + \frac{Q^2_{\mathrm{abs}}}{\tilde{T}^2_{\mathrm{reg}}} = 0 , \tag{2}$$

$$R_1 \begin{cases} Q^1_{\mathrm{reg}} + Q^1_{\mathrm{abs}} = \Delta Q , \\ \dfrac{Q^1_{\mathrm{reg}}}{\tilde{T}^1_{\mathrm{reg}}} + \dfrac{Q^1_{\mathrm{abs}}}{\tilde{T}^1_{\mathrm{abs}}} = \Delta S , \end{cases} \qquad R_2 \begin{cases} Q^2_{\mathrm{reg}} + Q^2_{\mathrm{abs}} = \Delta Q \\ \dfrac{Q^2_{\mathrm{reg}}}{\tilde{T}^2_{\mathrm{reg}}} + \dfrac{Q^2_{\mathrm{abs}}}{\tilde{T}^2_{\mathrm{abs}}} = - \Delta S . \end{cases} \tag{3}$$

With internal heat recovery, the coefficient of performance (COP) is

$$\mathrm{COP} = \frac{\dfrac{1}{\tilde{T}^2_{\mathrm{abs}}} - \dfrac{1}{\tilde{T}^2_{\mathrm{reg}}}}{\dfrac{1}{\tilde{T}^1_{\mathrm{reg}}} - \dfrac{1}{\tilde{T}^1_{\mathrm{abs}}}} \left[1 + \frac{\Delta Q}{Q^2_{\mathrm{reg}}} \left(\frac{\dfrac{1}{\tilde{T}^2_{\mathrm{abs}}} - \dfrac{1}{\tilde{T}^1_{\mathrm{abs}}}}{\dfrac{1}{\tilde{T}^2_{\mathrm{abs}}} - \dfrac{1}{\tilde{T}^2_{\mathrm{reg}}}} \right) \right] ,$$

$$\mathrm{COP} = \frac{1 - \dfrac{\tilde{T}^2_{\mathrm{abs}}}{\tilde{T}^2_{\mathrm{reg}}}}{\dfrac{\tilde{T}^1_{\mathrm{abs}}}{\tilde{T}^1_{\mathrm{reg}}} - 1} + \frac{\Delta S}{Q^2_{\mathrm{reg}}} \frac{\tilde{T}^1_{\mathrm{abs}} - \tilde{T}^2_{\mathrm{abs}}}{\dfrac{\tilde{T}^1_{\mathrm{abs}}}{\tilde{T}^2_{\mathrm{reg}}} - 1} = \mathrm{COP}\ c^{4\tilde{T}} + \frac{\Delta S}{Q^2_{\mathrm{reg}}} \frac{\tilde{T}^1_{\mathrm{abs}} - \tilde{T}^2_{\mathrm{abs}}}{\dfrac{\tilde{T}^1_{\mathrm{abs}}}{\tilde{T}^1_{\mathrm{reg}}} - 1} . \tag{4}$$

The objective of this work is experimental verification of the possibility in principle of advancing the multisalt reactor process using the physical adsorption of an active carbon fiber and chemical reactions of salts in the same reactor at the same time. It has been shown [3] that physical adsorption of ammonia by an active carbon fiber and ammonia absorption by $CaCl_2$ in the same reactor increase the adsorption capacity by at least two orders of magnitude. Internal heat recovery in a multisalt reactor and external heat recovery by a heat-pipe heat exchanger can be realized in transfer from high-temperature chemical salt pairs in the absorber phase to low-temperature pairs in the desorption phase. The COP of such a system will be higher than for a simple system without heat recovery.

The active carbon fiber Busofit with a high permeability, porosity, and capillary potential is used in this work as a fast sorbent bed and a host material for different salts. This carbon fiber provides a uniform distribution of thin (2–3 μ) films of salt on the porous host material surface.

The two basic phenomena of physical adsorption (Busofit) and chemical reaction (salts) are realized in the same reactor [4]. The carbon fiber Busofit as a fast sorbent material reacts with ammonia in the early stage of the heating/cooling time (up to 5 min), increasing the pressure in the reactor, and then the salts begin to react as a very effective sorbent bed. Busofit as a capillary-porous host material stimulates the distribution of the thin salt film throughout the entire volume of the sorbent bed during the regeneration time (ammonia capillary condensation, liquid motion through the sorbent bed due to the action of capillary forces). Due to its high permeability the use of Busofit is also suitable for sorption cycles coupled with forced-convection heating/cooling.

In conventional thermochemical cycles the main entropy production in resorption systems is due to superheating of vapor during the cold-production phase and de-superheating of vapor during the regeneration phase, and the main part of the reaction is used for pressurization and de-pressurization of the reactors. In our

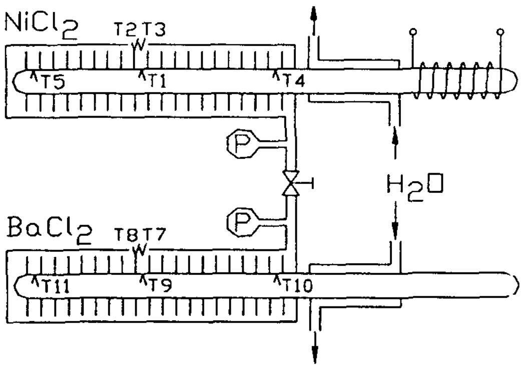

Fig. 1. Two-reactor configuration.

case Busofit acts as a rapidly reacting material that decreases the pressure drop between the cold-production and regeneration phases, thereby increasing the COP of the system. During the regenerating and cold-production phases there is a strong interaction between Busofit and the salts, the ammonia migrating from Busofit to the salts and back. This phenomenon is not yet fully understood and needs further investigation.

Description of the System. To verify the theoretical analysis for two-salt resorption systems some preliminary tests with two small reactors configured as a heat pump and cross-over valves were made (Fig. 1). The configuration is made up of two adsorbers (active carbon fiber, salts, and ammonia) with an interconnecting valve between them. Low-temperature adsorber No. 1 was filled with the active carbon fiber Busofit (mass 60 g) saturated with $BaCl_2$ (mass 60 g). High-temperature adsorber No. 2 was filled with the active carbon fiber Busofit (mass 65 g) saturated with $NiCl_2$ (mass 70 g).

Low-temperature adsorber No. 1 is heated/cooled with a heat-transfer device – a heat pipe (HFC as the working fluid). Similarly, high-temperature adsorber No. 2 is heated/cooled with a heat pipe (water as the working fluid).

Transient results. The temperature field and the pressure inside each adsorber were measured and recorded as a function of time. The optimum mass of ammonia inside the system was 56 g, which means that at room temperature most of the ammonia mass was concentrated in high-temperature absorber No. 2, and the equilibrium pressure in the system was 1.4 bar. In the time interval $\Delta\tau_1 = 30$ min the heat flow was supplied to adsorber No. 2 through a 100-W heat pipe. The temperature variation inside the sorbent bed (shown in Fig. 2 for thermocouples positioned at 1-5) followed the ammonia desorption and the ammonia transfer from adsorber No. 2 to low-temperature adsorber No. 1 and the ammonia adsorption inside the sorbent bed. The maximum temperature drop inside the sorbent bed, adsorber No. 2, was less than 40 ^{o}C. The temperature evolution inside the low-temperature sorbent bed (adsorber No. 1) is shown in Fig. 2 (for thermocouples positioned at 7-11). The temperature drop inside this sorbent bed was less than 1 ^{o}C due to the very efficient two-phase heat transfer of ammonia. The temperature $T_{\max}$ of the sorbent bed in adsorber No. 2 (Busofit + $NiCl_2$) was 240 ^{o}C. The temperature $T_{\max}$ of the sorbent bed in the adsorber No. 1 (Busofit + $BaCl_2$) was 50 ^{o}C. The temperature of the low-temperature sorbent bed (Busofit + $BaCl_2$) decreased (Fig. 2) from $T = 28$ ^{o}C to $T = 0$ ^{o}C in 3 min and then was constant for 7 min.

In the time interval $\Delta\tau_2 = 10$ min the temperature of the heat pipe (adsorber No. 2) was maintained constant 240 ^{o}C, and cooling water ($T = 18$ ^{o}C) was supplied to the heat exchanger of the heat pipe (adsorber No. 1) and the sorbent-bed temperature decreased to 28 ^{o}C.

In the time interval $\Delta\tau_3 = 10$ min the cooling-water circulation through the heat-pipe heat exchanger (adsorber No. 1) was cut, and this water was supplied to the high-temperature heat-pipe heat exchanger (adsorber No. 2). There was a sharp temperature decrease inside the sorbent bed from $T = 240$ ^{o}C to 130 ^{o}C in 3 minutes (with a temperature drop inside the sorbent bed of 40 ^{o}C), and subsequently the temperature field in the sorbent bed remained nearly constant for 7 min.

In the time interval $\Delta\tau_4 = 10$ min there was constant water circulation in the heat-pipe heat exchanger (adsorber No. 2, the temperature of the sorbent bed is 80 ^{o}C) and cooling. In this time interval the temperature of low water was supplied to the low-temperature heat-pipe heat exchanger (adsorber No. 1) to heat the sorbent bed to the temperature $T = 18$ ^{o}C. With this the first cycle of the functional experimental setup was completed.

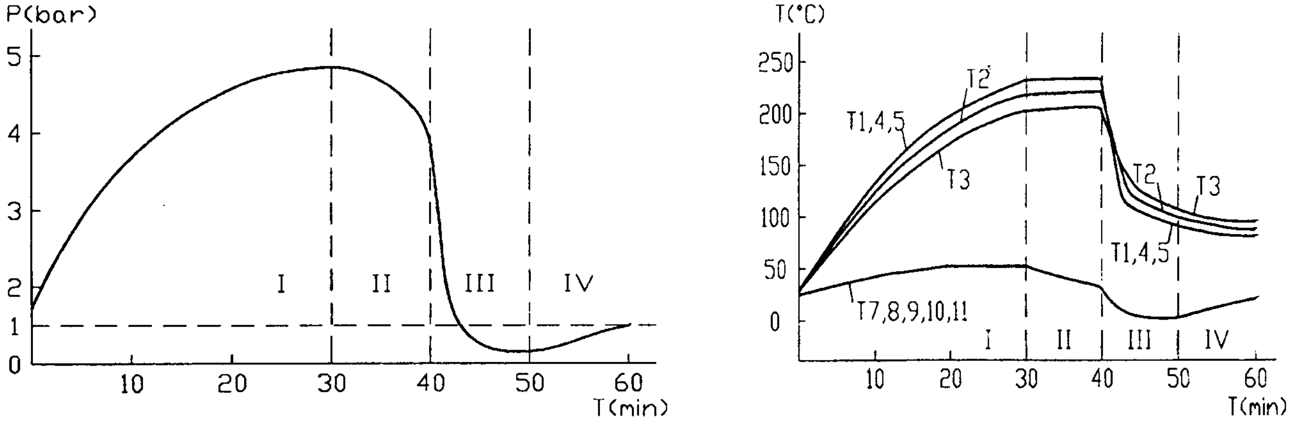

Fig. 2. Transient pressure and temperature profiles.

There is an ammonia pressure dependence inside the setup as a function of time (4 time intervals) (Fig. 2). The maximum pressure was about 8 bar (ammonia desorption inside the high-temperature sorbent bed), and the minimum ammonia pressure was 0.3 bar (ammonia adsorption inside the high-temperature sorbent bed). The long cycle time is due to the absence of insulation on the adsorbers and on the low-efficiency electric heater (on the heat-pipe surface). The COP of the system was 1.43 here.

These tests gave positive results from the point of view of confirming a high-temperature lift capability and stable operation of the system. The salt-gas couples for the reactor geometry are based on known and already tested salts – the chlorides $NiCl_2$, $MnCl_2$, $BaCl_2$. To improve the COP we incorporated the internal heat recovery streams using heat pipes. Application of the first and second laws of thermodynamics to a three-salt system gives us the possibility of analyzing the efficiency of the combinations $BaCl_2$ and $MnCl_2$, $BaCl_2$ and $NiCl_2$.

These two combination work in parallel in the desorption and adsorption modes. The first- and second-law analysis is made based on the following model of J. Castaing-Lasvignottes and P. Neveu. The influence of the internal irreversibilities and the external heat recovery through the heat-transfer systems (the heat pipes) is not considered:

$$Q^1_{\mathrm{reg}} + Q^1_{\mathrm{abs}} + Q^2_{\mathrm{reg}} + Q^2_{\mathrm{abs}} + Q^3_{\mathrm{reg}} + Q^3_{\mathrm{abs}} = 0\,,$$

$$Q^1_{\mathrm{reg}}/T^1_{\mathrm{reg}} + Q^1_{\mathrm{abs}}/T^1_{\mathrm{abs}} + Q^2_{\mathrm{reg}}/T^2_{\mathrm{reg}} +$$

$$+ Q^2_{\mathrm{abs}}/T^2_{\mathrm{abs}} + Q^3_{\mathrm{reg}}/T^3_{\mathrm{reg}} + Q^3_{\mathrm{abs}}/T^3_{\mathrm{abs}} + \Delta_f S = 0\,.$$

Supposing that the internal irreversibilities are negligible and that the external irreversibilities are expressed by

$$\Delta_f S^{\mathrm{ext}} = \Sigma\left[\int \delta q_i/T - 1/T_i \int \delta q_i\right]$$

and introducing the definition of the entropic temperature as

$$T^* = \frac{\int \delta q_i}{\int \delta q_i/T}\,,$$

the system becomes

$$Q^1_{\mathrm{reg}} + Q^1_{\mathrm{ads}} + Q^2_{\mathrm{reg}} + Q^2_{\mathrm{ads}} + Q^3_{\mathrm{reg}} + Q^3_{\mathrm{ads}} = 0\,,$$

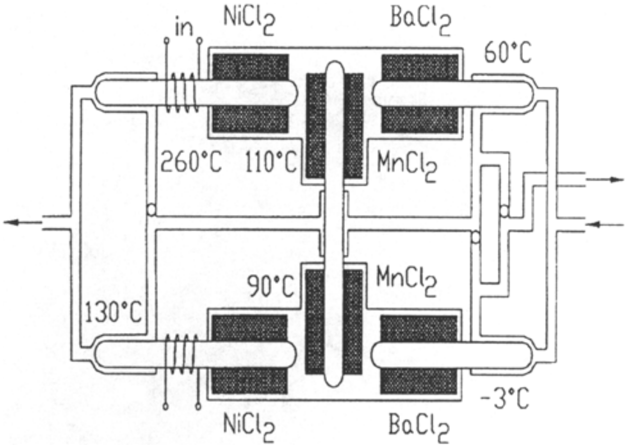

Fig. 3. Three-salt chemical cooler/heater.

$$\frac{Q^1_{\mathrm{reg}}}{T^1_{\mathrm{reg}}} + \frac{Q^1_{\mathrm{ads}}}{T^1_{\mathrm{ads}}} + \frac{Q^2_{\mathrm{reg}}}{T^2_{\mathrm{reg}}} + \frac{Q^2_{\mathrm{ads}}}{T^2_{\mathrm{ads}}} + \frac{Q^3_{\mathrm{reg}}}{T^3_{\mathrm{reg}}} + \frac{Q^3_{\mathrm{ads}}}{T^3_{\mathrm{ads}}} = 0 .$$

This can be written, combining the two subsystems, as:

subsystem R_1:

$$[Q^1_{\mathrm{reg}} + Q^1_{\mathrm{ads}} + Q^2_{\mathrm{reg}} + Q^2_{\mathrm{ads}} = \Delta Q] ,$$

$$\left[\frac{Q^1_{\mathrm{reg}}}{T^1_{\mathrm{reg}}} + \frac{Q^1_{\mathrm{ads}}}{T^1_{\mathrm{ads}}} + \frac{Q^2_{\mathrm{reg}}}{T^2_{\mathrm{reg}}} + \frac{Q^2_{\mathrm{ads}}}{T^2_{\mathrm{ads}}} = \Delta S\right] ,$$

subsystem R_2:

$$[Q^3_{\mathrm{reg}} + Q^3_{\mathrm{ads}} = - \Delta Q] ,$$

$$\left[\frac{Q^3_{\mathrm{reg}}}{T^3_{\mathrm{reg}}} + \frac{Q^3_{\mathrm{ads}}}{T^3_{\mathrm{ads}}} = - \Delta S\right] .$$

A resorption internal heat recovery system (3S/G) (Fig. 3) requires two identical branches of the reactors (a high-temperature reactor and a mean-temperature reactor); one is connected to a low-temperature reactor in the case where there is a synthesis reaction, and the other branch of the reactors is connected to another low-temperature reactor in the case where there is a decomposition reaction. The thermodynamic "thermosyphon" and the heat-transfer fluid loop provide heat exchange between the reactor sets. This thermal regeneration permits recovering up to 75-80% of the energy stored in the reactor, and the internal regeneration of the energy in one reactor with three salts thereby allows minimization of the mass and an increase in the reliability of the system with a reduced cycle.

The cooler system setup is composed of three different salts in six reactors with heat recovery.

The cycle is separated into two main phases corresponding to two pressure levels. During the low-pressure phase reactors No. 2 ($NiCl_2$ + $MnCl_2$) absorb (an exothermic reaction) the heat from the low-temperature source of heat ($BaCl_2$), while reactors No. 1 ($NiCl_2$ + $MnCl_2$) regenerate (an endothermic reaction) internal energy, as a result of which the second one tend toward the first. Therefore reactors No. 2 are connected to a thermal sink, typically the ambient at an intermediate temperature (TM), and produce cold at a low temperature (TL).

When the two reactions are complete, the system has to be regenerated (that is, prepared for a new cold-production phase).

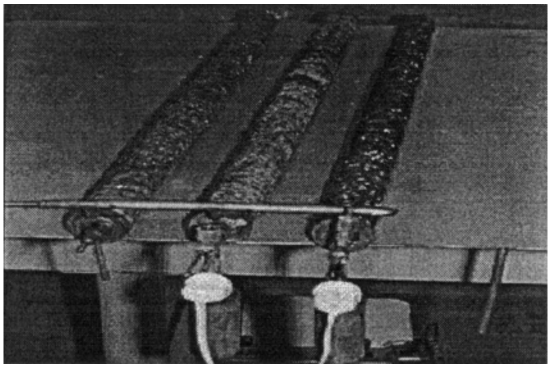

Fig. 4. Photograph of three sorbent beds of Busofit saturated with $NiCl_2$, $MnCl_2$, and $BaCl_2$ salts.

As regards system optimization, the three-salt reactors under consideration can meet the temperature lift requirements of designs based on a resorption architecture.

Conclusions. The conclusions are summarized as follows:

- The operation of a new three-salt-carbon chemical heat pump was experimentally verified.
- A heat output of 1.5 kW was tested with a temperature lift near $100^{o}C$ with a COP equal to 1.44 without heat recovery.
- With heat-pipe heat recovery the COP of this system can be increased to 1.62.
- The efficiency of this heat pump can be increased if for the bottom cycle a condenser and a capillary pumped evaporator are used.
- To increase the cycle efficiency it is necessary to improve the design of the adsorber, increase the number of salts with different temperature lifts, and use a convective mode for sorbent-bed heating.
- A four-salt heat pump could potentially be used to increase the COP of the system further, provided other parasitic losses can be reduced.

Finally the advantage of no moving parts makes this cooler/heater attractive for space and domestic applications.

REFERENCES

1. E. Lepinasse and B. Spinner, Production de Froid par couplage de reacteurs solide–gaz, Revue Internationale du Froid, 17, No. 5 (1994).
2. P. Neveu and J. Castaing-Lasvignottes, Second law analysis of advanced solid–gas chemical refrigerators, in: 1997 Int. Heat Powered Cycles Conf., Univesity of Nottingham, UK, 15-17 September 1997, 113-128 (1997).
3. E. Lepinasse et al., Modeling and experimental investigation of a new type of thermochemical transformer based on the coupling of two solid–gas reactions, Chemical Engineering and Processing, 33, 125-134 (1994).
4. B. Spinner, Les transformateurs thermochimiques a ammoniac, CNRS-IMP, Universite de Perpignan. 1996.
5. Proceedings of Ab-Sorption '96 Conference, 1, II, III, Sept. 1996, Montreal.
6. U. Rockenfeller and L. Kirol, Refrigerating recycling systems, US Patent No. 5,165,247 of Nov. 24 (1992).
7. B. Spinner, D. Stitou, and P. Grini, Cascading sorption machines: new concept for the power control of solid–gas thermochemical systems, in: Proc. Ab-Sorption '96, Montreal, Sept. 17-20, 1996, Vol. 2, 531-538 (1996).
8. L. L. Vasiliev, L. E. Kanonchik, A. A. Antuh, and A. G. Kulakov, NaX Zeolite, Carbon Fiber and $CaCl_2$, Ammonia Reactors for Heat Pumps and Refrigerators, in: Adsorption 2, 311-316 (1996).